Error analysis of a variational multiscale stabilization for convection-dominated diffusion equations in two dimensions

GUANGLIAN LI
Institut für Numerische Simulation, Universität Bonn, Wegelerstraße 6, D-53115 Bonn, Germany
li@ins.uni-bonn.de

AND

DANIEL PETERSEIM* AND MIRA SCHEDENSACK
Institut für Mathematik, Universität Augsburg, Universitätsstr. 14, D-86159 Augsburg, Germany
*Corresponding author: daniel.peterseim@math.uni-augsburg.de;
mira.schedensack@math.uni-augsburg.de

We formulate a stabilized quasi-optimal Petrov–Galerkin method for singularly perturbed convection–diffusion problems based on the variational multiscale method. The stabilization is of Petrov–Galerkin type with a standard finite element trial space and a problem-dependent test space based on pre-computed fine-scale correctors. The exponential decay of these correctors and their localization to local patch problems, which depend on the direction of the velocity field and the singular perturbation parameter, are rigorously justified. Under moderate assumptions, this stabilization guarantees stability and a quasi-optimal rate of convergence for arbitrary mesh Péclet numbers on fairly coarse meshes at the cost of additional inter-element communication.

Keywords: convection dominated; variational multiscale method; Petrov–Galerkin.

1. Introduction

Given a domain $\Omega \subset \mathbb{R}^2$, a singular perturbation parameter $0 < \epsilon \leq 1$, a velocity field $b \in (L^\infty(\Omega))^2$ and some force $f \in H^{-1}(\Omega)$, the convection–diffusion equation seeks $u \in V := H^1_0(\Omega)$ such that

$$\begin{aligned} -\epsilon \Delta u + b \cdot \nabla u &= f \quad \text{in } \Omega, \\ u &= 0 \quad \text{on } \partial\Omega. \end{aligned} \tag{1.1}$$

We assume that the velocity field b is incompressible, i.e., $\nabla \cdot b = 0$. The focus of this article is the convection-dominated regime with large Péclet number $\mathrm{Pe} = \|b\|_{L^\infty(\Omega)}/\epsilon$. For reasonably small Péclet numbers, classical Galerkin finite element methods (FEMs) perform well. However, if the Péclet number increases then steep gradients of u occur and boundary layers appear, requiring a much finer mesh to capture the characteristic width of these boundary layers. Consequently, local corrections are needed at the layers and a numerical method in which the smooth solution regions are not polluted by the layers is desirable. The thickness of the parabolic layer is $\mathcal{O}(\sqrt{\epsilon})$ and $\mathcal{O}(\epsilon)$ for the exponential layer, which have to be resolved for a stable approximation with a standard Galerkin FEM. Furthermore, it holds that

$|u|_{H^1(\Omega^*)} = \mathcal{O}(\epsilon^{-1/4})$ and $|u|_{H^1(\Omega^o)} = \mathcal{O}(\epsilon^{-1/2})$ with small neighborhoods Ω^* and Ω^o of the parabolic and the exponential boundary layer, respectively (Roos *et al.*, 2008; John & Schmeyer, 2009).

Numerous numerical methods have been proposed in the past few decades aimed at solving the convection-dominated problem (1.1) efficiently and accurately. Upwinding methods for stabilization of the exponential boundary layers combined with refinement near the parabolic boundary layers are formulated. Among them are the streamline upwind/Petrov–Galerkin (SUPG) method or Galerkin least squares (GLS) method (Franca *et al.*, 1992; Christiansen *et al.*, 2016), *hp* finite element methods (Melenk, 1997, 2002), discontinuous Petrov–Galerkin methods (Demkowicz *et al.*, 2012), residual-free bubble (RFB) approaches (Brezzi *et al.*, 2000; Cangiani & Süli, 2005a,b), methods with an additional nonlinear diffusion (Barrenechea *et al.*, 2016), methods with stabilization by local orthogonal sub scales (Codina, 2000) and hybridizable discontinuous Galerkin methods (Qiu & Shi, 2015). Among the multiscale methods are variational multiscale (VMS) methods (Hughes & Sangalli, 2007; Larson & Målqvist, 2009), multiscale finite element methods (Park & Hou, 2004; Calo *et al.*, 2016), multiscale hybrid-mixed methods (Harder *et al.*, 2015) and local orthogonal decomposition (LOD) methods (Elfverson, 2015). Specifically, the residual-based stabilization methods (SUPG, GLS and RFB) incorporate global stability properties into high accuracy in local regions away from the boundary layers. We refer to Roos *et al.* (2008) for an overview of robust numerical methods for singular perturbed problems. In this article, our focus is on the construction and the error analysis of a stable and accurate LOD method based on Hughes & Sangalli (2007), Peterseim (2017) and Målqvist & Peterseim (2011).

VMS methods were designed for solving multiscale problems by embedding fine-scale information into a coarse-scale framework. Essentially, the efficiency and accuracy rely on the construction of a problem-dependent stable projector from a larger fine space onto a relatively much smaller coarse space. Our motivation for this article originates from Hughes & Sangalli (2007), where the authors derived an explicit formula for the one-dimensional fine-scale Green's function arising in VMS methods. The smaller the support of the fine-scale Green's function, the more favorable the localized method (e.g., Målqvist & Peterseim, 2011; Peterseim, 2017) in solving (1.1). In particular, the authors compared the fine-scale Green's functions derived by the L^2-projector with that derived by the H_0^1-projector and concluded that the latter outweighed the former in the one-dimensional case. In addition, examples were shown for the two-dimensional case that the H_0^1-projector would exceed the L^2-projector as well. There is a recent work (Elfverson, 2015) on the convection–diffusion problem employing the L^2-projector in the framework of the VMS and LOD methods. The author shows convergence of the localized method and tests the method using the H_0^1-projector and claims that the superiority of the H_0^1-projector over the L^2-projector is not valid for the two-dimensional case. This claim is supported by Fig. 2 below.

In the one-dimensional case, the H_0^1-projection equals the nodal interpolation. Therefore, another possible generalization of the one-dimensional case to higher dimensions is to use nodal interpolation in the VMS method. Doing this, we take into account that nodal interpolation is not well defined and stable as an operator on H^1 functions. After regularization using a very fine reference discretization of scale $h \lesssim \epsilon$, the use of nodal interpolation can be justified as the stability constant degenerates with $\log(H/h)$ in two dimensions only (see (3.1) below). This approach was previously utilized in Larson & Målqvist (2009) and is shown to work better than averaging-type operators in the regime of large mesh Péclet numbers (see Fig. 2 below). In this article, we show that a VMS method based on the nodal interpolation operator coupled with a Petrov–Galerkin method is stable and locally quasi-optimal for the convection-dominated problem (1.1) with no spurious oscillations and no smearing. As for other elliptic partial differential equations (PDEs), the ideal VMS method is turned into a practical method by localizing the support of the VMS basis functions (Peterseim 2016b). Inspired by the numerical results of the fine-scale Green's functions displayed in Hughes & Sangalli (2007) and the proof in our article as well, a *b*-biased local

region is proposed as the numerical domain for approximating the ideal method. The convergence of this localization is proved under the assumption that the local region is sufficiently large. In three dimensions, the method is still applicable, but the instability of nodal interpolation is more severe and the size of the subdomains may be prohibitively large to compensate this negative effect.

The remainder of this article is organized as follows. In Section 2, a detailed description of the problem considered in this article is shown. In Section 3, we propose a new VMS method based on the nodal interpolation and denote it as the ideal method. Its stability and local quasi-optimality are displayed. In Section 4, we estimate the error of the global correctors outside a certain local patch and show an exponential decay of the error with respect to the size of the local patch. Inspired by the results in Section 4, we formulate the localization algorithm in Section 5 for the ideal method proposed in Section 3 and display the stability of this algorithm as well as the convergence. A numerical experiment is provided in Section 6 for the validation of our method and we conclude this article with conclusions in Section 7.

2. Model problem and standard finite elements

We assume that the parameter $\epsilon \leq 1$ and $b \in L^\infty(\Omega;\mathbb{R}^2)$ is a divergence-free vector field and we define the bilinear form a on $V \times V$ associated to (1.1) by

$$a(u,v) = \epsilon \int_\Omega \nabla u \cdot \nabla v \, \mathrm{d}x + \int_\Omega (b \cdot \nabla u)\, v \, \mathrm{d}x \qquad \text{for all } u, v \in V. \tag{2.1}$$

Because $\nabla \cdot b = 0$, an integration by parts implies that the bilinear form a is V-elliptic, i.e.,

$$a(v,v) = \epsilon \, |v|^2_{H^1(\Omega)} \qquad \text{for all } v \in V. \tag{2.2}$$

Furthermore, a Poincaré–Friedrichs inequality leads to the existence of some constant $C(\Omega, b)$ that may depend on (the diameter of) the domain Ω and the L^∞ norm of b such that a is continuous, i.e., for all $u, v \in V$ it holds that

$$\begin{aligned} a(u,v) &\leq \epsilon \, |u|_{H^1(\Omega)} \, |v|_{H^1(\Omega)} + \|b\|_{L^\infty(\Omega)} \, |u|_{H^1(\Omega)} \, \|v\|_{L^2(\Omega)} \\ &\leq C(\Omega, b) \, |u|_{H^1(\Omega)} \, |v|_{H^1(\Omega)} . \end{aligned} \tag{2.3}$$

Here, we used that $\epsilon \leq 1$. Throughout this article, $A \lesssim B$ abbreviates that there exists a constant $C > 0$ independent of ϵ, h and H (h and H will be defined later), such that $A \leq CB$, and let $A \gtrsim B$ be defined as $B \lesssim A$, and $A \approx B$ abbreviates $A \lesssim B \lesssim A$. We assume that $\|b\|_{L^\infty(\Omega)} \approx 1$. Let $\langle \bullet, \bullet \rangle_{H^{-1}(\Omega)\times H^1_0(\Omega)}$ denote the dual pairing of $H^{-1}(\Omega)$ and $H^1_0(\Omega)$.

We consider the variational form of (1.1):

$$\begin{cases} \text{find } u \in V \text{ such that for all } v \in V \\ a(u,v) = \langle f, v \rangle_{H^{-1}(\Omega)\times H^1_0(\Omega)}. \end{cases} \tag{2.4}$$

By virtue of the V-ellipticity and V-continuity of a from (2.2) and (2.3) and the Lax–Milgram lemma, problem (2.4) has a unique solution in V.

Let $\mathcal{T}_h$ be a shape-regular triangulation of the domain Ω, where h represents the minimal diameter of all triangles in $\mathcal{T}_h$. Given a triangulation $\mathcal{T}$, let

$$\mathcal{P}_1(\mathcal{T}) := \{v \in C^0(\Omega) \mid v|_K \in P^1(K) \text{ for all } K \in \mathcal{T}\}$$

denote the space of piecewise linear finite elements and define $V_h := \mathcal{P}_1(\mathcal{T}_h) \cap V$.

Let $u_h \in V_h$ denote the reference solution, which is defined as the Galerkin approximation that satisfies

$$a(u_h, v_h) = \langle f, v_h \rangle_{H^{-1}(\Omega)\times H_0^1(\Omega)} \qquad \text{for all } v_h \in V_h. \tag{2.5}$$

Taking advantage of the ellipticity and continuity of a from (2.2) and (2.3) on $V \times V \supset V_h \times V_h$, the Lax–Milgram lemma implies that the fine-scale solution u_h of (2.5) exists and is unique on V_h.

We assume that $\epsilon \ll 1$ is a small parameter and that $\mathcal{T}_h$ resolves ϵ in the sense that u_h is a good approximation of u, e.g., if

$$h_{\max}\|b\|_{L^\infty(\Omega)}/\epsilon \lesssim 1 \tag{2.6}$$

with the maximal mesh size $h_{\max}$ of $\mathcal{T}_h$. It holds that

$$|u - u_h|_{H^1(\Omega)} \lesssim \left(1 + \frac{h_{\max}\|b\|_{L^\infty(\Omega)}}{\epsilon}\right) \inf_{v_h \in V_h} |u - v_h|_{H^1(\Omega)}.$$

If, in addition, the solution u of (2.4) satisfies $u \in H^2(\Omega)$, standard interpolation estimates lead to

$$|u - u_h|_{H^1(\Omega)} \lesssim h_{\max}\left(1 + \frac{h_{\max}\|b\|_{L^\infty(\Omega)}}{\epsilon}\right)\|u\|_{H^2(\Omega)},$$

with a hidden constant independent of ϵ. Note, however, that $\|u\|_{H^2(\Omega)}$ depends on ϵ.

3. The ideal method

In this section, we introduce a variational multiscale method based on nodal interpolation, which yields a locally best approximation of the reference solution $u_h \in V_h$ from (2.5) and which is computed on a feasible coarse underlying mesh $\mathcal{T}_H$. We assume that $\mathcal{T}_H$ is a regular quasi-uniform triangulation of the domain Ω with maximal mesh size H, such that $\mathcal{T}_h$ is a refinement of $\mathcal{T}_H$. Let $\mathcal{N}_H$ denote the nodes in $\mathcal{T}_H$ and mid_K the barycenter for each coarse element $K \in \mathcal{T}_H$. The maximal mesh size H of $\mathcal{T}_H$ represents a computationally feasible scale that is typically much larger than ϵ. Altogether, the target regime is then

$$0 < h < \epsilon \ll H \lesssim 1.$$

Define $V_H = \mathcal{P}_1(\mathcal{T}_H) \cap V$ and let $I_H : V_h \to V_H$ denote the nodal interpolation. Note that I_H acts only on finite element functions and is, hence, well defined. It holds

$$H^{-1}\|v - I_H v\|_{L^2(T)} + |I_H v|_{H^1(T)} \le C_{I_H}\left(\tfrac{H}{h}\right)|v|_{H^1(T)}. \tag{3.1}$$

Indeed, we have (Yserentant 1986)

$$C_{I_H}\left(\frac{H}{h}\right) \lesssim \begin{cases} 1 & \text{in one dimension,} \\ \log \frac{H}{h} & \text{in two dimensions,} \\ \frac{H}{h} & \text{in three dimensions.} \end{cases}$$

Given $v_H \in V_H$, define the subscale corrector $\mathcal{C} : V_H \to \operatorname{Ker} I_H$ by

$$a(w, \mathcal{C}v_H) = a(w, v_H) \qquad \text{for all } w \in \operatorname{Ker} I_H. \tag{3.2}$$

The well-posedness of (3.2) follows from the ellipticity and continuity of a, as $\operatorname{Ker} I_H \subset V$.

Now we are ready to define the multiscale test space as

$$W_H := (1 - \mathcal{C})V_H.$$

Note that (3.2) implies that

$$W_H = \{w \in V_h : \forall\, v \in \operatorname{Ker} I_H, a(v, w) = 0\}.$$

The Petrov–Galerkin method for the approximation of (2.5) based on the trial–test pairing (V_H, W_H) defined above seeks $u_H \in V_H$ satisfying

$$a(u_H, w_H) = \langle f, w_H \rangle_{H^{-1}(\Omega)\times H_0^1(\Omega)} \qquad \text{for all } w_H \in W_H. \tag{3.3}$$

Note that (3.3) is a variational characterization of I_H in the sense that, for all $w_H \in W_H$, we have

$$a(I_H u_h, w_H) = a(I_H u_h - u_h, w_H) + a(u_h, w_H) = (f, w_H),$$

where the last equality follows from (3.2), (2.5) and the fact that $I_H u_h - u_h \in \operatorname{Ker} I_H$. As $\dim V_H = \dim W_H$, it follows that $u_H = I_H u_h \in V_H$ is the unique solution of (3.3) and the ideal method inherits favorable stability and approximation properties from the interpolation I_H. To be more precise, we have the following proposition, which follows directly from the identity $u_H = I_H u_h$ and (3.1).

PROPOSITION 3.1 (Stability and local quasi-optimality of the ideal method) For any $f \in H^{-1}(\Omega)$, the ideal Petrov–Galerkin method (3.3) admits a unique solution u_H in the standard finite element space V_H. The method is stable in the sense that

$$|u_H|_{H^1(\Omega)} \le C_{I_H}\left(\frac{H}{h}\right) |u_h|_{H^1(\Omega)},$$

where $u_h \in V_h$ denotes the reference solution that solves (2.5). Note that the constant $C_{I_H}\left(\frac{H}{h}\right)$ is independent of ϵ but may depend on H/h.

Moreover, for any $T \in \mathcal{T}_H$, we have the local best approximation result

$$|u_h - u_H|_{H^1(T)} \le C_{I_H}\left(\frac{H}{h}\right) \min_{v_H \in V_H} |u_h - v_H|_{H^1(T)}.$$

REMARK 3.2 The stability and quasi-optimality of Proposition 3.1 also holds for any other norm in which I_H is stable.

We admit that the corrector problems (3.2) are global problems on the fine triangulation $\mathcal{T}_h$, which have to be precomputed for solving (3.3). This would result in a number, $\dim(V_H)$, of problems of dimension $\mathcal{O}(\dim(V_h))$, which is comparable to solving the original problem (1.1) on a fine grid by an efficient standard method. This makes the VMS method (3.3) not realistic. However, it can be observed in Fig. 1 that the corrector of functions with local support are still quasi-local in the sense that they decay exponentially. This allows for an approximation of the corrector by functions of local support. In the next section, the exponential decay will be made rigorous, whereas Section 5 proves stability and approximation properties for a localization strategy.

REMARK 3.3 (Justification of choice of nodal interpolation) In other applications (Elfverson, 2015; Gallistl & Peterseim, 2015; Målqvist & Peterseim, 2011; Peterseim, 2016b, 2017), the method is usually based on stable quasi-interpolation operators rather than nodal interpolation. This is also possible here and would prevent the constant $C_{I_H}\big(\frac{H}{h}\big)$ from depending on h and, hence, ϵ. However, in the localization step, this choice of nodal interpolation turns out to be crucial and leads to very fast decay in all directions but downstream. In particular, it prevents any spread in the cross-stream and upstream direction as it is observed for averaging-type operators and the H^1_0-projector. This is illustrated in Fig. 2, which shows the decay behavior of a test basis function for several interpolation operators.

We conclude this section with a proof of stability in the classical inf–sup sense, although the method is perfectly stable in the sense of Proposition 3.1. This result will be used in Section 5 to prove well-posedness of the localized version of (3.3).

LEMMA 3.4 (Stability) The trial–test pairing (V_H, W_H) satisfies the inf–sup condition

$$\inf_{w_H\in W_H\setminus\{0\}}\sup_{u_H\in V_H\setminus\{0\}}\frac{a(u_H,w_H)}{|u_H|_{H^1(\Omega)}\,|w_H|_{H^1(\Omega)}}\geq\frac{\epsilon}{C_{I_H}\big(\frac{H}{h}\big)}. \tag{3.4}$$

Proof. Given $w_H\in W_H$, take $u_H=I_H(w_H)\in V_H$. Then by (3.1),

$$|u_H|_{H^1(\Omega)}\leq C_{I_H}\big(\tfrac{H}{h}\big)\,|w_H|_{H^1(\Omega)}\,. \tag{3.5}$$

Note that $I_H(w_H)-w_H\in\operatorname{Ker} I_H$. By (3.2), we have

$$a(u_H,w_H)=a(I_H(w_H),w_H)=a(w_H,w_H)=\epsilon\,|w_H|^2_{H^1(\Omega)}\,, \tag{3.6}$$

where the last inequality follows from $\nabla\cdot b=0$.

We obtain the result by the application of (3.5). □

4. Exponential decay of element correctors

This section is devoted to the proof of the exponential decay of element correctors defined in the following. Given $\omega\subset\Omega$, define the local bilinear form

$$a_\omega(u,v):=\epsilon\int_\omega\nabla u\cdot\nabla v\,\mathrm{d}x+\int_\omega(b\cdot\nabla u)\,v\,\mathrm{d}x\qquad\text{for all } u,v\in V \tag{4.1}$$

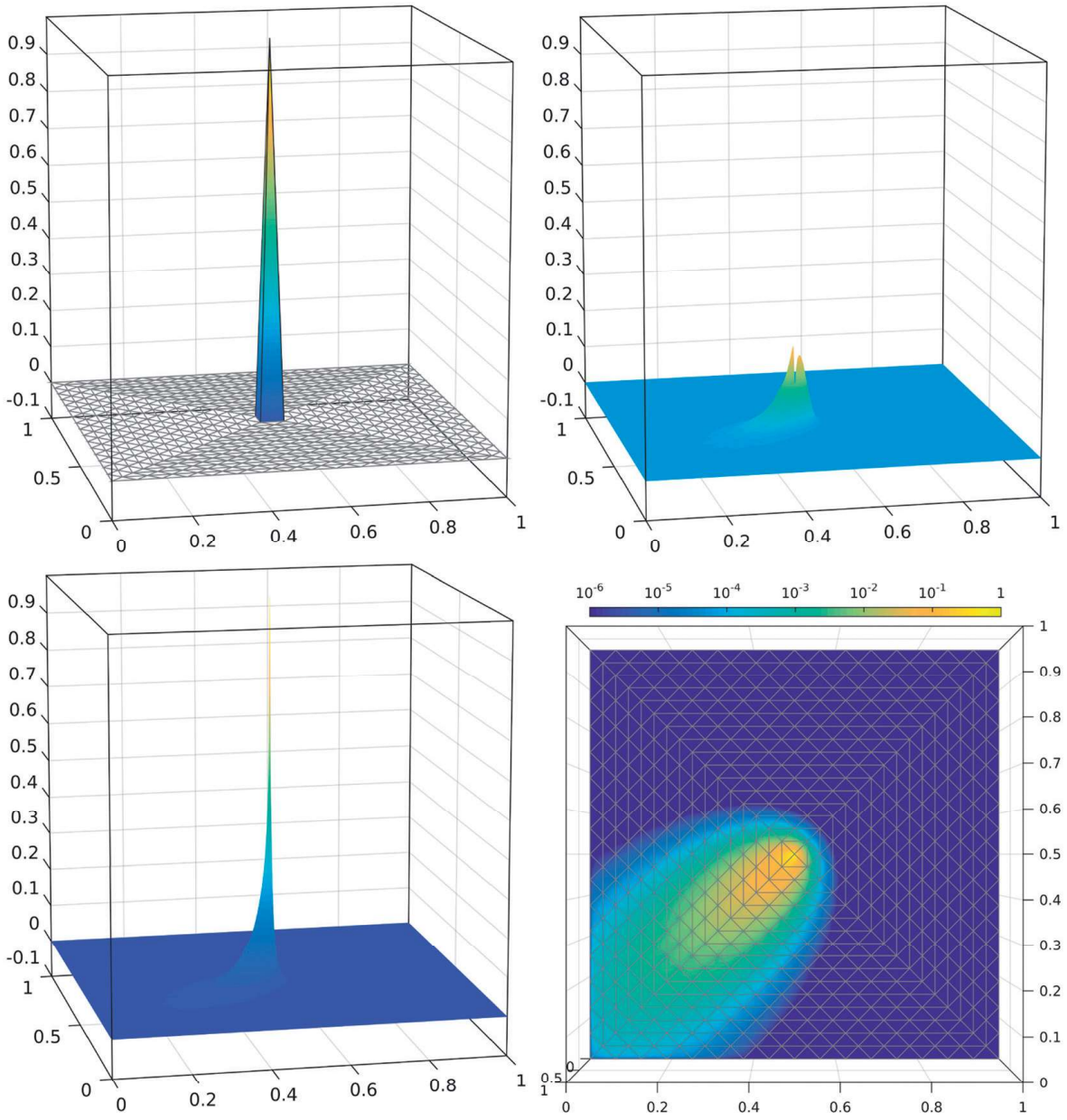

FIG. 1. Standard nodal basis function λ_z with respect to the coarse mesh $\mathcal{T}_H$ (top left), corresponding ideal corrector $\mathcal{C}\lambda_z$ (top right) and corresponding test basis function $(1-\mathcal{C})\lambda_z$ (bottom left). The bottom right figure shows a top view of the modulus of the test basis function $(1-\mathcal{C})\lambda_z$ with logarithmic color scale to illustrate the exponential decay property. The underlying data are $b = [\cos(0.7), \sin(0.7)]$ and $\epsilon = 2^{-7}$.

and let the local corrector $\mathcal{C}_T : V_H \to \operatorname{Ker} I_H$ be defined for any $v_H \in V_H$ by

$$a(w, \mathcal{C}_T v_H) = a_T(w, v_H) \qquad \text{for all } w \in \operatorname{Ker} I_H. \tag{4.2}$$

Note that $\mathcal{C} = \sum_{T\in\mathcal{T}_H} \mathcal{C}_T$ holds for the corrector $\mathcal{C}$ defined by (3.2).

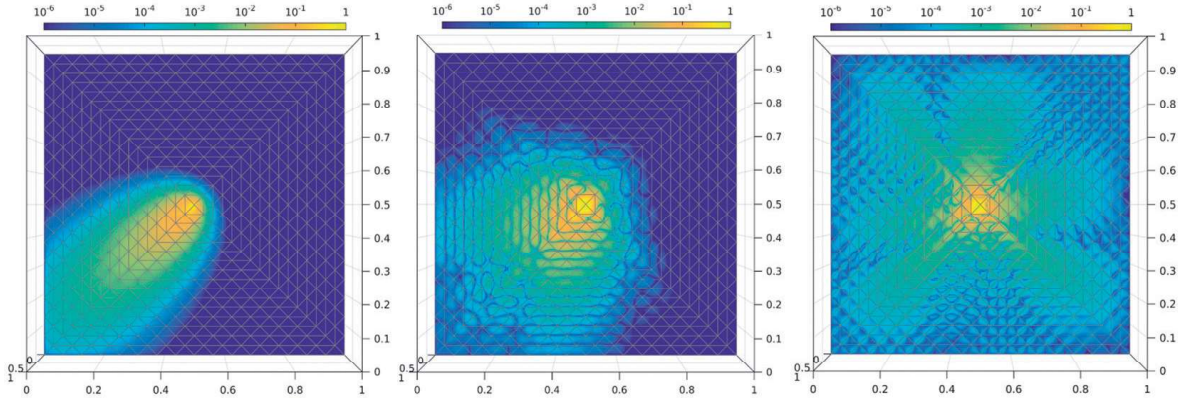

FIG. 2. Impact of the choice of interpolation operator on the decay of the ideal test basis function $(1 - \mathcal{C})\lambda_z$ in the underresolved regime $H \gg \epsilon$: nodal interpolation (left), L^2-projection (middle) and H_0^1-projection (right). The underlying data are $b = [\cos(0.7), \sin(0.7)]$ and $\epsilon = 2^{-7}$.

We consider the case that $\epsilon \leq H$. In the following, we restrict ourselves to a constant vector field b and w.l.o.g. $|b| = 1$; see Remark 4.4 below for a discussion for nonconstant vector fields b. Define t as a unit vector in $\mathbb{R}^2$, such that $t \cdot b = 0$. Define a rectangle $S_{T,\ell,b}$ for each $T \in \mathcal{T}_H$ and $\ell \in \mathbb{N}_+$ by

$$\begin{aligned} S_{T,\ell,b} := \Omega \cap \operatorname{conv}\{&\operatorname{mid}_T - \ell H t + \ell H b, \operatorname{mid}_T + \ell H t + \ell H b, \\ &\operatorname{mid}_T - \ell H t - \ell H^2 b/\epsilon, \operatorname{mid}_T + \ell H t - \ell H^2 b/\epsilon\}. \end{aligned} \tag{4.3}$$

We do not assume that b is aligned with the triangulation, and therefore, we define the patches $\Omega_{T,\ell,b}$ by

$$\Omega_{T,\ell,b} := \cup\{T' \in \mathcal{T}_H \mid T' \cap S_{T,\ell,b} \neq \emptyset\} \supset S_{T,\ell,b}.$$

See Fig. 3 for an illustration. For fixed $\ell \in \mathbb{N}_+$, the element patches have finite overlap in the sense that there exists a constant $C_{\mathrm{ol},\ell}(\epsilon) > 0$, such that

$$\max_{K \in \mathcal{T}_H} \#\{T \in \mathcal{T}_H \mid K \subset \Omega_{T,\ell,b}\} \leq C_{\mathrm{ol},\ell}(\epsilon). \tag{4.4}$$

THEOREM 4.1 Let $T \in \mathcal{T}_H$ and $v_H \in V_H$ and let $\mathcal{C}_T v_H$ denote the corresponding local subscale corrector as defined in (4.2). Then, we have

$$|\mathcal{C}_T v_H|_{H^1(\Omega \setminus S_{T,\ell,b})} \lesssim \beta^\ell \, |\mathcal{C}_T v_H|_{H^1(\Omega)}. \tag{4.5}$$

The constant β reads

$$\beta = \left(\frac{4C_{I_H}\left(\frac{H}{h}\right) + 3C_{I_H}\left(\frac{H}{h}\right)^2}{1 + 4C_{I_H}\left(\frac{H}{h}\right) + 3C_{I_H}\left(\frac{H}{h}\right)^2} \right)^{1/2} < 1 \tag{4.6}$$

and is bounded away from 1.

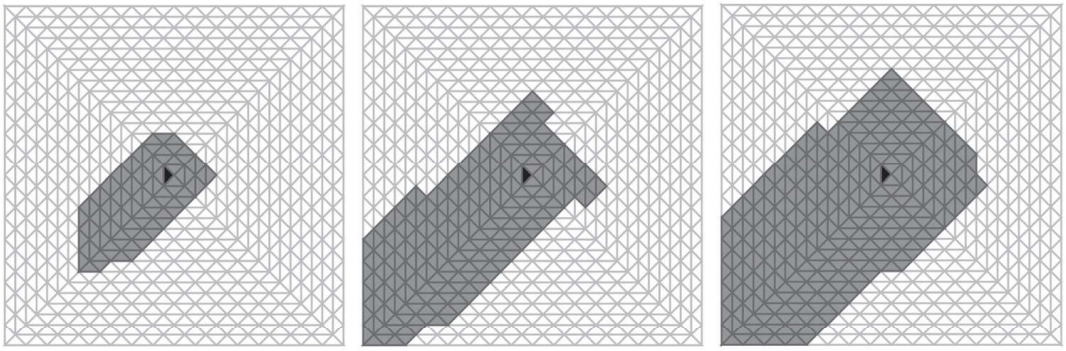

FIG. 3. Element patches $\Omega_{T,\ell,b}$ for $b = [\cos(0.7), \sin(0.7)]$, $\epsilon = 2^{-7}$ and $\ell = 1, 2, 3$ (from left to right) as they are used in the localized corrector problem (5.1).

Before going to the proof of this theorem, we express the exponential decay in terms of patches in the following corollary. This is a direct consequence of Theorem 4.1 and the definition of $\Omega_{T,\ell,b}$.

COROLLARY 4.2 Let $T \in \mathcal{T}_H$ and $v_H \in V_H$ and let $\mathcal{C}_T v_H$ denote the corresponding local subscale corrector as defined in (4.2). Then, we have

$$|\mathcal{C}_T v_H|_{H^1(\Omega\setminus\Omega_{T,\ell,b})} \leq |\mathcal{C}_T v_H|_{H^1(\Omega\setminus S_{T,\ell,b})} \lesssim \beta^\ell \, |\mathcal{C}_T v_H|_{H^1(\Omega)} \tag{4.7}$$

with $\beta < 1$ from (4.6).

REMARK 4.3 Recall that in this two-dimensional situation, $C_{I_H}\left(\frac{H}{h}\right) \lesssim \log(\frac{H}{h})$ for $C_{I_H}\left(\frac{H}{h}\right)$ from (3.1). Then given fixed $H \in (0, 1)$ and let $h \to 0$, the constant β scales as

$$1 - \beta^2 \gtrsim \frac{1}{1 + \log(h)^2}.$$

In the three-dimensional case, Theorem 4.1 could essentially be proven in the same way, but the dependence of $C_{I_H}\left(\frac{H}{h}\right)$ on H/h is algebraic, so that the decay rate deteriorates very fast.

Proof of Theorem 4.1. The crucial point in the proof is (4.10) below, which exploits the direction of b. This allows for patches that are only enlarged in the direction of $-b$. The remaining part of the proof then essentially follows as in Målqvist & Peterseim (2011).

Define a cutoff function

$$\eta := 1 - \eta_1 \eta_2,$$

where $0 \leq \eta_1(x) \leq 1$ and $0 \leq \eta_2(x) \leq 1$ are one-dimensional continuous piecewise affine cutoff functions along t and b, respectively. Recall that mid_T denotes the barycenter of a coarse element T, $|b| = 1$ and t is a unit vector orthogonal to b. We define η_1 and η_2 by

$$\eta_1(x) = \begin{cases} 1 & \text{if } |(x - \text{mid}_T) \cdot t| \leq (\ell - 1)H, \\ 0 & \text{if } |(x - \text{mid}_T) \cdot t| \geq \ell H \end{cases} \tag{4.8}$$

and

$$\eta_2(x) = \begin{cases} 1 & \text{if } -(\ell-1)H \le -(x-\mathrm{mid}_T)\cdot b \le (\ell-1)\dfrac{H^2}{\epsilon}, \\ 0 & \text{if } -(x-\mathrm{mid}_T)\cdot b \ge \ell\dfrac{H^2}{\epsilon} \text{ or } -(x-\mathrm{mid}_T)\cdot b \le -\ell H. \end{cases} \tag{4.9}$$

We obtain from the construction above that $\nabla\eta_1(x)\cdot b = 0$ for all $x \in \Omega$ and $\eta_1 \le 1$. Moreover, because $-(b\cdot\nabla\eta_2(x)) \le 0$ if $0 \le (x-\mathrm{mid}_T)\cdot b$, we deduce

$$-b\cdot\nabla\eta = -(b\cdot\nabla\eta_1)\eta_2 - (b\cdot\nabla\eta_2)\eta_1 = -(b\cdot\nabla\eta_2)\eta_1 \le \frac{\epsilon}{H^2}. \tag{4.10}$$

Furthermore, $\eta|_{S_{T,\ell-1,b}} = 0$ and $\eta|_{\Omega\setminus S_{T,\ell,b}} = 1$, and η is bounded between 0 and 1 and satisfies the Lipschitz continuity

$$\|\nabla\eta\|_{L^\infty(\Omega)} \le 2/H. \tag{4.11}$$

Note that $\mathrm{supp}(\nabla\eta) \subset S_{T,\ell,b} \setminus S_{T,\ell-1,b}$.

Let $(\bullet,\bullet) := (\bullet,\bullet)_{L^2(\Omega)}$ denote the L^2 scalar product and define $\varphi := \mathcal{C}_T v_H$. As $\nabla\cdot b = 0$, we have $(b\cdot\nabla(\eta\varphi),\eta\varphi) = 0$, and

$$\begin{aligned} \epsilon\,|\varphi|^2_{H^1(\Omega\setminus S_{T,\ell,b})} &\le \epsilon(\nabla(\eta\varphi),\nabla(\eta\varphi)) + (b\cdot\nabla(\eta\varphi),\eta\varphi) \\ &= \epsilon(\nabla\varphi,\eta\nabla(\eta\varphi)) + \epsilon(\nabla\eta,\varphi\nabla(\eta\varphi)) + (b\cdot\nabla(\eta\varphi),\eta\varphi) \\ &= \epsilon(\nabla\varphi,\nabla(\eta^2\varphi)) + (b\cdot\nabla(\eta^2\varphi),\varphi) - \epsilon(\nabla\varphi,\eta\varphi\nabla\eta) \\ &\quad + \epsilon(\nabla\eta,\varphi\nabla(\eta\varphi)) - (b\cdot\nabla\eta,\eta\varphi^2). \end{aligned}$$

Observe that $\eta^2\varphi \in \mathrm{Ker}\, I_H$, and we obtain

$$\epsilon(\nabla\varphi,\nabla(\eta^2\varphi)) + (b\cdot\nabla(\eta^2\varphi),\varphi) = a(\eta^2\varphi,\varphi) = a_T(\eta^2\varphi,v_H) = 0 \tag{4.12}$$

by the definition of $\mathcal{C}_T$ in (4.2). Thus, we arrive at

$$\epsilon\,|\varphi|^2_{H^1(\Omega\setminus S_{T,\ell,b})} \le \epsilon|(\nabla\varphi,\eta\varphi\nabla\eta)| + \epsilon|(\nabla\eta,\varphi\nabla(\eta\varphi))| - (b\cdot\nabla\eta,\eta\varphi^2). \tag{4.13}$$

We will estimate each term on the right-hand side of (4.13). With $\eta \le 1$ and (4.11), a Cauchy inequality leads to

$$\begin{aligned} \epsilon|(\nabla\varphi,\eta\varphi\nabla\eta)| &\le 2\epsilon H^{-1}\,|\varphi|_{H^1(S_{T,\ell,b}\setminus S_{T,\ell-1,b})}\,\|\varphi\|_{L^2(S_{T,\ell,b}\setminus S_{T,\ell-1,b})} \\ &\le 2C_{I_H}\!\left(\tfrac{H}{h}\right)\epsilon\,|\varphi|^2_{H^1(S_{T,\ell,b}\setminus S_{T,\ell-1,b})}, \end{aligned}$$

where we have used the fact that $\varphi \in \mathrm{Ker}\, I_H$ and estimate (3.1) in the last inequality.

The same arguments imply for the second term in (4.13),

$$\begin{aligned}\epsilon|(\nabla\eta,\varphi\nabla(\eta\varphi))| &\le 2\epsilon H^{-1}\,\|\varphi\|_{L^2(S_{T,\ell,b}\setminus S_{T,\ell-1,b})}\,|\eta\varphi|_{H^1(S_{T,\ell,b}\setminus S_{T,\ell-1,b})}\\ &\le 2\epsilon\left(C_{I_H}\left(\tfrac{H}{h}\right)^2+C_{I_H}\left(\tfrac{H}{h}\right)\right)|\varphi|^2_{H^1(S_{T,\ell,b}\setminus S_{T,\ell-1,b})}.\end{aligned}$$

The crucial point in the estimation of the last term in (4.13) is estimate (4.10), which implies together with $\eta\varphi^2\ge 0$,

$$\begin{aligned}-(b\cdot\nabla\eta,\eta\varphi^2) &\le \frac{\epsilon}{H^2}\,\|\varphi\|^2_{L^2(S_{T,\ell,b}\setminus S_{T,\ell-1,b})}\\ &\le \epsilon C_{I_H}\left(\tfrac{H}{h}\right)^2|\varphi|^2_{H^1(S_{T,\ell,b}\setminus S_{T,\ell-1,b})}.\end{aligned}$$

Assemble all estimates above for (4.13) to conclude

$$\epsilon\,|\varphi|^2_{H^1(\Omega\setminus S_{T,\ell,b})}\le\epsilon\left(4C_{I_H}\left(\tfrac{H}{h}\right)+3C_{I_H}\left(\tfrac{H}{h}\right)^2\right)|\varphi|^2_{H^1(S_{T,\ell,b}\setminus S_{T,\ell-1,b})}.$$

Define $C\left(\frac{H}{h}\right):=4C_{I_H}\left(\frac{H}{h}\right)+3C_{I_H}\left(\frac{H}{h}\right)^2$, which leads to

$$|\varphi|^2_{H^1(\Omega\setminus S_{T,\ell,b})}\le C\left(\tfrac{H}{h}\right)\left(|\varphi|^2_{H^1(\Omega\setminus S_{T,\ell-1,b})}-|\varphi|^2_{H^1(\Omega\setminus S_{T,\ell,b})}\right),$$

and therefore

$$|\varphi|^2_{H^1(\Omega\setminus S_{T,\ell,b})}\le\frac{C\left(\frac{H}{h}\right)}{1+C\left(\frac{H}{h}\right)}\,|\varphi|^2_{H^1(\Omega\setminus S_{T,\ell-1,b})}.$$

Repeating this process, we arrive at

$$|\varphi|^2_{H^1(\Omega\setminus S_{T,\ell,b})}\le\left(\frac{C\left(\frac{H}{h}\right)}{1+C\left(\frac{H}{h}\right)}\right)^{\ell}|\varphi|^2_{H^1(\Omega)}.$$

This concludes the proof. □

REMARK 4.4 (Nonconstant b) If the velocity field b is divergence-free, but not globally constant, the definition of the rectangles $S_{T,\ell,b}$ has to be modified in that they have to follow the velocity. To avoid the computation of those patches for a complicated b, one may alternatively enlarge the patches adaptively using *a posteriori* error estimators (Larson & Målqvist, 2009).

The following sketch shows that the proof of the exponential decay can be generalized to the situation where there exists a bounded diffeomorphism with bounded inverse that maps a constant reference velocity field b_{ref} to b, in the following sense. Assume that there exists a reference domain Ω_{ref} and a diffeomorphism $\psi:\Omega_{\text{ref}}\to\Omega$, $\psi\in\mathcal{C}^1(\Omega_{\text{ref}})$, such that

$$D\psi(y)b_{\text{ref}}=b(\psi(y))\qquad\text{for all } y\in\Omega_{\text{ref}},$$

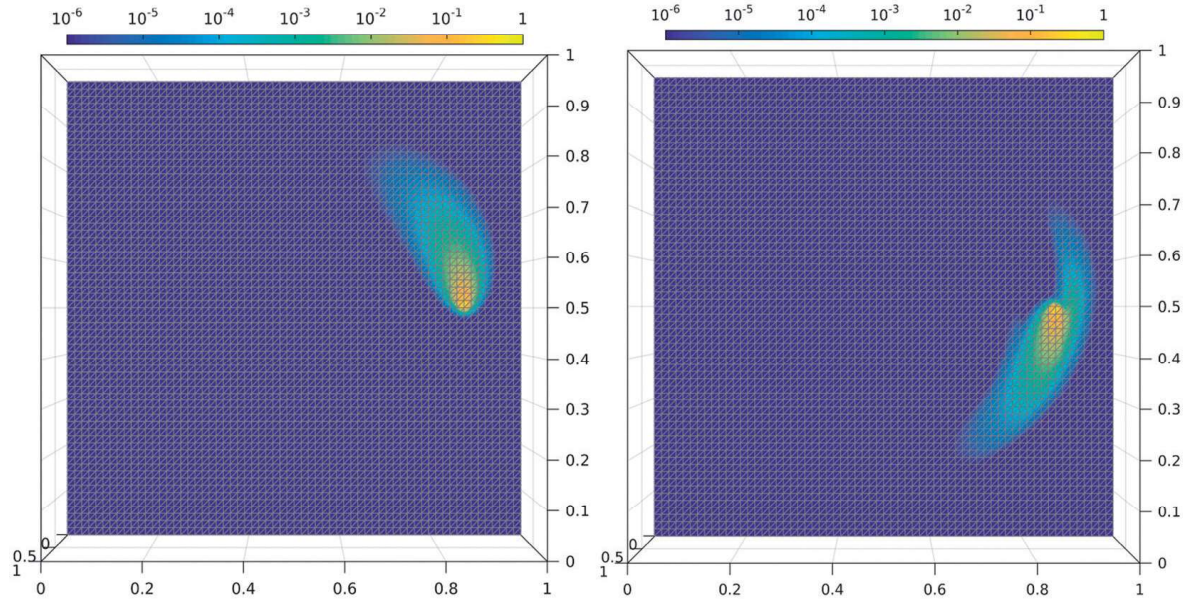

FIG. 4. Top view of the modulus of (ideal) test basis functions $(1 - \mathcal{C})\lambda_z$ with a logarithmic color scale. The underlying data are $\epsilon = 2^{-8}$ and b_1 (left) and b_2 (right) from (4.14).

i.e., ψ follows b in the following sense. For any $y_{0,\mathrm{ref}} \in \Omega_{\mathrm{ref}}$, the function $y(t) := \psi(y_{0,\mathrm{ref}} + tb_{\mathrm{ref}})$ solves the ordinary differential equation (ODE) $y'(t) = b(y(t))$, i.e., y follows b.

The domain $S_{T,\ell,b}$ (formerly a rectangle) is then defined as $S_{T,\ell,b} := \psi(S_{\mathrm{ref},T,\ell,b_{\mathrm{ref}}})$, where $S_{\mathrm{ref},T,\ell,b_{\mathrm{ref}}} \subset \Omega_{\mathrm{ref}}$ is defined for the constant vector field b_{ref} as in (4.3). The cutoff function $\eta = 1 - \eta_1\eta_2$ is then defined by $\eta_j(x) := \eta_{j,\mathrm{ref}}(\psi^{-1}(x))$ for $\eta_{j,\mathrm{ref}}$ defined as in (4.8)–(4.9). The boundedness of $D\psi^{-1}$ then proves

$$\|\nabla\eta\|_{L^\infty(\Omega)} \lesssim H^{-1}.$$

The definitions of η_1 and η_2 lead for all $x \in \Omega$ to

$$b(x) \cdot \nabla\eta_j(x) = \nabla\eta_{j,\mathrm{ref}}|_{\psi^{-1}(x)} \cdot (D\psi^{-1}(x)b(x)) = \nabla\eta_{j,\mathrm{ref}}|_{\psi^{-1}(x)} \cdot b_{\mathrm{ref}},$$

which implies $-b \cdot \nabla\eta \le \epsilon/H^2$. Theorem 4.1 then follows as before.

Figure 4 displays the modified basis functions $(1 - \mathcal{C})\lambda_z$ for $z = (0.875, 0.5)$ for the following nonconstant vector fields

$$b_1(x) = 5\begin{pmatrix} x_2 - 0.5 \\ 0.5 - x_1 \end{pmatrix} \text{ and } b_2(x) = \left(2\left(\left\lceil x - \begin{pmatrix} 0.5 \\ 0.5 \end{pmatrix}\right\rceil - 1\right) \bmod 2\right) b_1(x), \tag{4.14}$$

where $\lceil r \rceil := \min\{k \in \mathbb{N} \mid k \ge r\}$ denotes the ceiling function. For the first example, there exists a diffeomorphism ψ as above in a subdomain $(0.6, 1) \times (0, 1)$, whereas for the second example, this is not true due to the jumps of b_2. Nevertheless, one observes a typical exponential decay pattern that follows b very closely.

5. LOD method and error analysis

On the basis of the results above, we conclude that the energy norm of $\mathcal{C}_T v$ decreases very fast outside a local region around T for any $v \in V_H$. Therefore, a localization process is feasible to reduce the computational costs of the ideal method but maintain a good accuracy. In this section, we want to localize the corrector problems (3.2). To this end, instead of solving them on the global domain Ω, we obtain a good approximation of those correctors by solving a local problem on $\Omega_{T,\ell,b}$.

First, let us introduce some notation. In the following, we will denote $R_H = \operatorname{Ker} I_H$ and $R_H(\Omega_{T,\ell,b}) = \{w \in R_H, \text{ and } w = 0 \text{ in } \Omega \setminus \Omega_{T,\ell,b}\}$. Recall the local bilinear form a_ω defined in (4.1). The localized element corrector $\mathcal{C}_{T,\ell} : V_H \to R_H(\Omega_{T,\ell,b})$ is defined as follows: given $v_H \in V_H$, let $\mathcal{C}_{T,\ell} v_H \in R_H(\Omega_{T,\ell,b})$ satisfy

$$a_{\Omega_{T,\ell,b}}(w, \mathcal{C}_{T,\ell} v_H) = a_T(w, v_H) \qquad \text{for all } w \in R_H(\Omega_{T,\ell,b}). \tag{5.1}$$

Then we denote $\mathcal{C}_\ell := \sum_{T \in \mathcal{T}_H} \mathcal{C}_{T,\ell}$; see Fig. 5 for an illustration of the localized correctors $\mathcal{C}_\ell \lambda_z$ and the corresponding localized test basis.

In the following lemma, we will show that $\mathcal{C}_{T,\ell}$ is a good approximation of $\mathcal{C}_T$ provided that the local patches $\Omega_{T,\ell,b}$ are sufficiently large. For ease of presentation, we denote the mesh Péclet number $\mathrm{Pe}_{H,b,\epsilon}$ of $\mathcal{T}_H$ by

$$\mathrm{Pe}_{H,b,\epsilon} := H \|b\|_{L^\infty(\Omega)} / \epsilon. \tag{5.2}$$

Recall the definition of β from (4.6).

LEMMA 5.1 Given $v \in V_H$ and $\ell \in \mathbb{N}_+$, it holds that

$$\left|\mathcal{C}_T v - \mathcal{C}_{T,\ell} v\right|_{H^1(\Omega)} \lesssim \left(1 + \mathrm{Pe}_{H,b,\epsilon}\, C_{I_H}\!\left(\tfrac{H}{h}\right)\right)^2 \left(C_{I_H}\!\left(\tfrac{H}{h}\right) + 1\right) \beta^{\ell-1} \left|v\right|_{H^1(T)}. \tag{5.3}$$

Proof. Define $e_{T,\ell} := \mathcal{C}_T v - \mathcal{C}_{T,\ell} v$. In view of $R_H(\Omega_{T,\ell,b}) \subset R_H$, the definitions of the correctors in (5.1) and (3.2) and the orthogonality of Petrov–Galerkin type lead to

$$\epsilon \left|e_{T,\ell}\right|^2_{H^1(\Omega)} = a(e_{T,\ell}, e_{T,\ell}) = a(e_{T,\ell} - w, e_{T,\ell}) \qquad \text{for all } w \in R_H(\Omega_{T,\ell,b}).$$

As $I_H(e_{T,\ell}) = 0$, Hölder's inequality and the approximation property (3.1) of I_H imply

$$\left|e_{T,\ell}\right|^2_{H^1(\Omega)} \le \left(1 + \mathrm{Pe}_{H,b,\epsilon}\, C_{I_H}\!\left(\tfrac{H}{h}\right)\right) \left|e_{T,\ell}\right|_{H^1(\Omega)} \left|e_{T,\ell} - w\right|_{H^1(\Omega)}.$$

As $w \in R_H(\Omega_{T,\ell,b})$ is arbitrary, we arrive at

$$\left|e_{T,\ell}\right|_{H^1(\Omega)} \le \left(1 + \mathrm{Pe}_{H,b,\epsilon}\, C_{I_H}\!\left(\tfrac{H}{h}\right)\right) \left|\mathcal{C}_T v - w\right|_{H^1(\Omega)}. \tag{5.4}$$

In the following, we construct a specific $w \in R_H(\Omega_{T,\ell,b})$ to control the term $|\mathcal{C}_T v - w|_{H^1(\Omega)}$. Let η denote the cutoff function from the proof of Theorem 4.1, such that $\eta|_{S_{T,\ell-1,b}} = 0$ and $\eta|_{\Omega \setminus S_{T,\ell,b}} = 1$. Note that $S_{T,\ell,b} \subset \Omega_{T,\ell,b}$ and therefore $\mu := 1 - \eta$ satisfies $\mu|_{\Omega \setminus \Omega_{T,\ell,b}} = 0$. In addition, μ is bounded between 0 and 1 and satisfies the Lipschitz continuity

$$\|\nabla \mu\|_{L^\infty(\Omega)} \le 2H^{-1}. \tag{5.5}$$

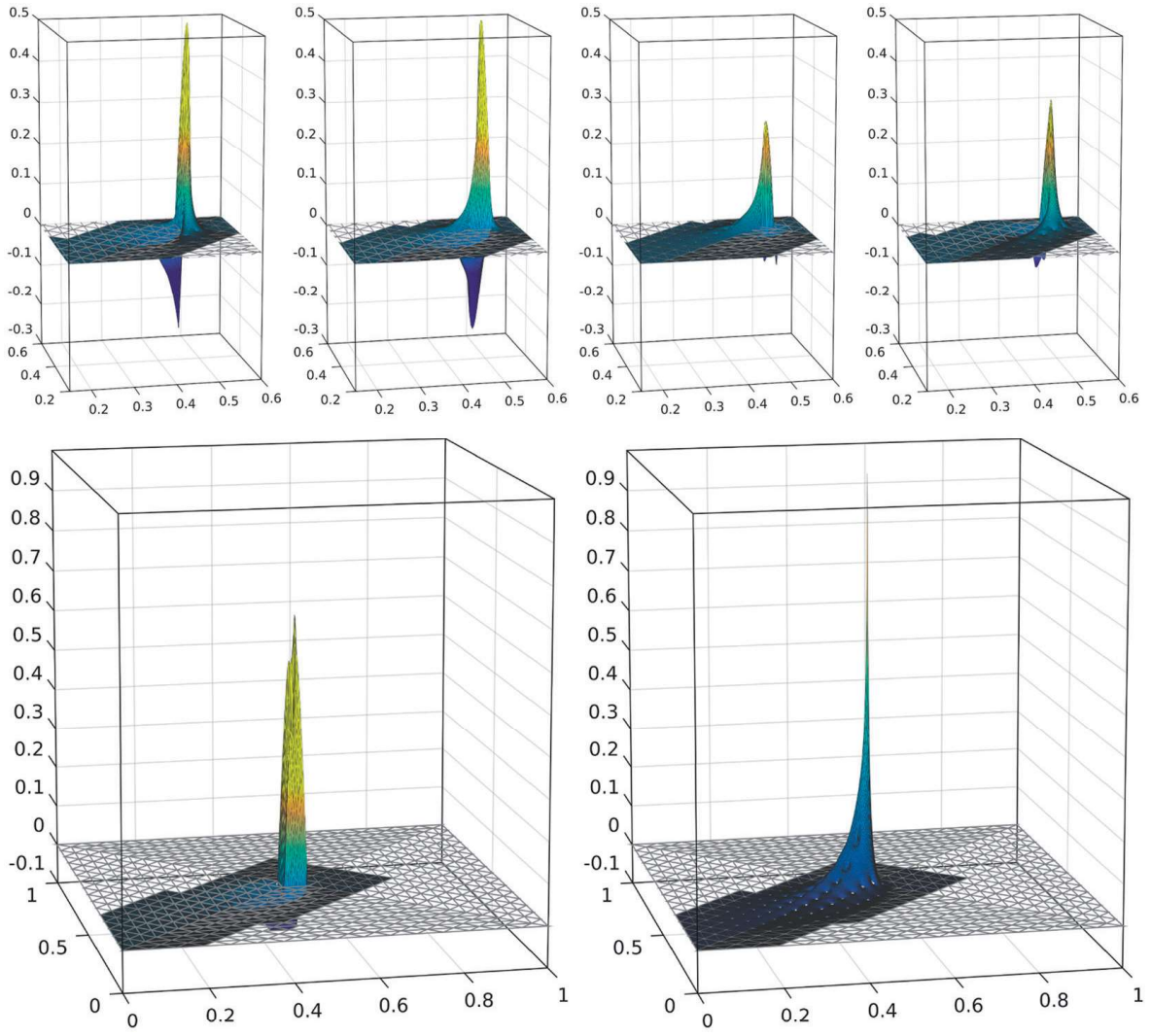

FIG. 5. Localized element correctors $\mathcal{C}_{T,\ell}\lambda_z$ for $\ell = 2$ and all four elements T adjacent to the vertex $z = [0.5, 0.5]$ (top), localized nodal corrector $\mathcal{C}_\ell\lambda_z = \sum_{T\ni z}\mathcal{C}_{T,\ell}\lambda_z$ (bottom left) and corresponding test basis function $(1-\mathcal{C}_\ell)\lambda_z$ (bottom right). The underlying data are $b = [\cos(0.7), \sin(0.7)]$ and $\epsilon = 2^{-7}$. The computations have been performed by standard linear finite elements on local fine meshes of width $h = 2^{-8}$. See Fig. 1 for a comparison with the ideal global corrector and basis.

Define $w = \mu\mathcal{C}_T v$; then $w \in R_H(\Omega_{T,\ell,b})$. As $\mathcal{C}_T v \in R_H$, the fact that $0 \le \mu \le 1$ and (5.5) lead as in the proof of Theorem 4.1 to

$$\begin{aligned}|\mathcal{C}_T v - w|_{H^1(\Omega)} &= |\mathcal{C}_T v - \mu\mathcal{C}_T v|_{H^1(\Omega\setminus S_{T,\ell-1,b})}\\ &\le 2(C_{I_H}\left(\tfrac{H}{h}\right)+1)\,|\mathcal{C}_T v|_{H^1(\Omega\setminus S_{T,\ell-1,b})}.\end{aligned}$$

Theorem 4.1 then implies

$$|\mathcal{C}_T v - w|_{H^1(\Omega)} \lesssim (C_{I_H}\left(\tfrac{H}{h}\right)+1)\beta^{\ell-1}\,|\mathcal{C}_T v|_{H^1(\Omega)}\,.$$

The combination with (5.4) implies

$$\left|\mathcal{C}_T v - \mathcal{C}_{T,\ell} v\right|_{H^1(\Omega)} \lesssim \left(1 + \mathrm{Pe}_{H,b,\epsilon}\, C_{I_H}\!\left(\tfrac{H}{h}\right)\right)\left(C_{I_H}\!\left(\tfrac{H}{h}\right) + 1\right)\beta^{\ell-1}\, |\mathcal{C}_T v|_{H^1(\Omega)}\,.$$

In the end, we show the stability of $\mathcal{C}_T$ to bound the term $|\mathcal{C}_T v|_{H^1(\Omega)}$. As $I_H(\mathcal{C}_T v) = 0$, the stability of $\mathcal{C}_T$ follows from

$$\begin{aligned}
\epsilon\, |\mathcal{C}_T v|^2_{H^1(\Omega)} &= a(\mathcal{C}_T v, \mathcal{C}_T v) = a_T(\mathcal{C}_T v, v) \\
&\le \epsilon\, |\mathcal{C}_T v|_{H^1(\Omega)}\, |v|_{H^1(T)} + \|b\|_{L^\infty(T)}\, |v|_{H^1(T)}\, \|\mathcal{C}_T v\|_{L^2(\Omega)} \\
&\le \left(\epsilon + H\|b\|_{L^\infty(T)} C_{I_H}\!\left(\tfrac{H}{h}\right)\right) |\mathcal{C}_T v|_{H^1(\Omega)}\, |v|_{H^1(T)}\,,
\end{aligned}$$

where the definition of the element corrector in (5.1) implies the second equality and the approximation property (3.1) leads to the last inequality. This proves the assertion. □

The following theorem assembles the local estimates from Lemma 5.1 to derive an estimate for the global corrector.

THEOREM 5.2 Given $v \in V_H$ and $\ell \in \mathbb{N}_+$, it holds that

$$|\mathcal{C} v - \mathcal{C}_\ell v|_{H^1(\Omega)} \lesssim C(H, h, \epsilon, b, \ell)\beta^{\ell-1}\, |v|_{H^1(\Omega)} \tag{5.6}$$

with

$$\begin{aligned}
C(H, h, \epsilon, b, \ell) := &\left(1 + \mathrm{Pe}_{H,b,\epsilon}\, C_{I_H}\!\left(\tfrac{H}{h}\right)\right)^2 \left(C_{I_H}\!\left(\tfrac{H}{h}\right) + 1\right) \\
&\times \left(1 + 2C_{I_H}\!\left(\tfrac{H}{h}\right) + \mathrm{Pe}_{H,b,\epsilon}\, C_{I_H}\!\left(\tfrac{H}{h}\right)\right) C_{\mathrm{ol},\ell+2}(\epsilon)^{1/2}.
\end{aligned} \tag{5.7}$$

Proof. Set $z := \mathcal{C} v - \mathcal{C}_{\ell-2} v \in \operatorname{Ker} I_H$ and $z_T := \mathcal{C}_T v - \mathcal{C}_{T,\ell-2} v$, then $z = \sum_{T \in \mathcal{T}_H} z_T$. We have

$$\epsilon\, |z|^2_{H^1(\Omega)} = \sum_{T \in \mathcal{T}_H} a(z, z_T). \tag{5.8}$$

We estimate $a(z, z_T)$ for each coarse element $T \in \mathcal{T}_H$. Recall that we defined a cutoff function η in the proof of Theorem 4.1. Note that $\Omega_{T,\ell-2,b} \subset S_{T,\ell-1,b}$. By construction, we have $\eta z \in R_H(\Omega \setminus S_{T,\ell-1,b}) \subset R_H(\Omega \setminus \Omega_{T,\ell-2,b})$. As $\mathcal{C}_{T,\ell-2} v|_{\Omega \setminus \Omega_{T,\ell-2,b}} = 0$, this implies

$$a(\eta z, z_T) = a(\eta z, \mathcal{C}_T v).$$

Furthermore, notice that $\eta z \in \ker(I_H)$, which combined with (4.2) yields

$$a(\eta z, \mathcal{C}_T v) = a_T(\eta z, v) = 0.$$

As a consequence, we obtain

$$a(z, z_T) = a(\eta z, z_T) + a((1-\eta) z, z_T) = a((1-\eta) z, z_T).$$

In the following, we will bound the term $a((1-\eta)z, z_T)$. Recall from the proof of Theorem 4.1 that $(1-\eta)|_{\Omega\setminus S_{T,\ell,b}} = 0$, $\|\nabla(1-\eta)\|_{L^\infty(\Omega)} \leq 2H^{-1}$ and $\|(1-\eta)\|_{L^\infty(\Omega)} \leq 1$. Taking into account that $I_H(z) = I_H(z_T) = 0$, the stability of the projector I_H from (3.1), therefore, leads to

$$\begin{aligned} a((1-\eta)z, z_T) &\leq \epsilon\, |(1-\eta)z|_{H^1(S_{T,\ell,b})}\, |z_T|_{H^1(S_{T,\ell,b})} + \|b\|_{L^\infty(\Omega)}\, \|z\|_{L^2(S_{T,\ell,b})}\, |z_T|_{H^1(S_{T,\ell,b})} \\ &\leq \left(\epsilon\left(1 + 2C_{I_H}\left(\tfrac{H}{h}\right)\right) + \|b\|_{L^\infty(\Omega)} H C_{I_H}\left(\tfrac{H}{h}\right)\right) |z|_{H^1(S_{T,\ell,b})}\, |z_T|_{H^1(S_{T,\ell,b})}\,. \end{aligned}$$

As $S_{T,\ell,b} \subset \Omega_{T,\ell,b}$, the combination with (5.8) and the application of a discrete Cauchy–Schwarz inequality yields

$$\begin{aligned} |z|^2_{H^1(\Omega)} &\leq \left(1 + 2C_{I_H}\left(\tfrac{H}{h}\right) + \mathrm{Pe}_{H,b,\epsilon}\, C_{I_H}\left(\tfrac{H}{h}\right)\right) \sum_{T\in\mathcal{T}_H} |z|_{H^1(S_{T,\ell,b})}\, |z_T|_{H^1(S_{T,\ell,b})} \\ &\leq \left(1 + 2C_{I_H}\left(\tfrac{H}{h}\right) + \mathrm{Pe}_{H,b,\epsilon}\, C_{I_H}\left(\tfrac{H}{h}\right)\right) \\ &\quad \times \left(\sum_{T\in\mathcal{T}_H} |z|^2_{H^1(\Omega_{T,\ell,b})}\right)^{1/2} \left(\sum_{T\in\mathcal{T}_H} |z_T|^2_{H^1(S_{T,\ell,b})}\right)^{1/2}. \end{aligned}$$

Lemma 5.1 implies

$$\left(\sum_{T\in\mathcal{T}_H} |z_T|^2_{H^1(S_{T,\ell,b})}\right)^{1/2} \lesssim \left(1 + \mathrm{Pe}_{H,b,\epsilon}\, C_{I_H}\left(\tfrac{H}{h}\right)\right)^2 \left(C_{I_H}\left(\tfrac{H}{h}\right) + 1\right) \beta^{\ell-3}\, |v|_{H^1(\Omega)}\,,$$

while the bounded overlap of the patches from (4.4) implies

$$\left(\sum_{T\in\mathcal{T}_H} |z|^2_{H^1(\Omega_{T,\ell,b})}\right)^{1/2} \leq C_{\mathrm{ol},\ell}(\epsilon)^{1/2}\, |z|_{H^1(\Omega)}\,.$$

In the end, the combination of the previously displayed inequalities and the shift $\ell \mapsto \ell + 2$ shows the assertion. □

Now we are ready to define the localized multiscale test space as

$$W_{H,\ell} = (1 - \mathcal{C}_\ell) V_H.$$

The Petrov–Galerkin method for the approximation of (2.5) based on the trial–test pairing $(V_H, W_{H,\ell})$ defined above seeks $u_{H,\ell} \in V_H$ satisfying

$$a(u_{H,\ell}, w_{H,\ell}) = \langle f, w_{H,\ell}\rangle_{H^{-1}(\Omega)\times H^1_0(\Omega)} \qquad \text{for all } w_{H,\ell} \in W_{H,\ell}. \tag{5.9}$$

LEMMA 5.3 (Inf–sup stability) If ℓ is sufficiently large, i.e., the oversampling condition

$$\ell \gtrsim \frac{1 + \left|\log\left(C_{I_H}\left(\frac{H}{h}\right)\right)\right| + \left|\log\left(C(H,h,\epsilon,b,\ell)\right)\right| + \left|\log\left(1 + C_{I_H}\left(\frac{H}{h}\right) + \mathrm{Pe}_{H,b,\epsilon}\, C_{I_H}\left(\frac{H}{h}\right)^2\right)\right|}{\left|\log\left(4C_{I_H}\left(\frac{H}{h}\right) + 3C_{I_H}\left(\frac{H}{h}\right)^2\right) - \log\left(1 + 4C_{I_H}\left(\frac{H}{h}\right) + 3C_{I_H}\left(\frac{H}{h}\right)^2\right)\right|} \tag{5.10}$$

is satisfied, then the Petrov–Galerkin method (5.9) is inf–sup stable and

$$\inf_{w_{H,\ell}\in W_{H,\ell}\setminus\{0\}} \sup_{u_H\in V_H\setminus\{0\}} \frac{a(u_H, w_{H,\ell})}{|u_H|_{H^1(\Omega)} \left|w_{H,\ell}\right|_{H^1(\Omega)}} \gtrsim \frac{\epsilon}{C_{I_H}\left(\frac{H}{h}\right)}. \tag{5.11}$$

REMARK 5.4 If $H/h = 1/\epsilon$ and $|b| = 1$ then (5.10) reads

$$\ell \gtrsim (\log(\epsilon))^2,$$

i.e., the local patch size ℓ depends on $\log(\epsilon)$ algebraically.

REMARK 5.5 As the dimension of V_H equals the dimension of $W_{H,\ell}$, the reverse inf–sup condition

$$\inf_{u_H\in V_H\setminus\{0\}} \sup_{w_{H,\ell}\in W_{H,\ell}\setminus\{0\}} \frac{a(u_H, w_{H,\ell})}{|u_H|_{H^1(\Omega)} \left|w_{H,\ell}\right|_{H^1(\Omega)}} \gtrsim \frac{\epsilon}{C_{I_H}\left(\frac{H}{h}\right)} \tag{5.12}$$

follows from Lemma 5.3.

Proof of Lemma 5.3. Let $w_{H,\ell} \in W_{H,\ell}$, and set $w_H = (1 - \mathcal{C})I_H w_{H,\ell} \in W_H$. By Lemma 3.4, there exists $u_H \in V_H$, such that

$$a(u_H, w_H) \geq \frac{\epsilon}{C_{I_H}\left(\frac{H}{h}\right)} |u_H|_{H^1(\Omega)} |w_H|_{H^1(\Omega)}. \tag{5.13}$$

Taking into account that $w_{H,\ell} = I_H w_{H,\ell} - \mathcal{C}_\ell I_H w_{H,\ell}$, we arrive at $w_H - w_{H,\ell} = (\mathcal{C}_\ell - \mathcal{C})I_H w_{H,\ell}$. As a consequence, Theorem 5.2 together with the stability of I_H from (3.1) implies

$$\begin{aligned}\left|w_H - w_{H,\ell}\right|_{H^1(\Omega)} &\leq \tilde{C}C(H,h,\epsilon,b,\ell)\beta^{\ell-1} \left|I_H w_{H,\ell}\right|_{H^1(\Omega)} \\ &\leq \tilde{C}C(H,h,\epsilon,b,\ell)C_{I_H}\left(\tfrac{H}{h}\right)\beta^{\ell-1} \left|w_{H,\ell}\right|_{H^1(\Omega)}.\end{aligned}$$

Here, $\tilde{C}$ denotes the constant hidden in $\lesssim$ in Theorem 5.2, which is independent of H, h or ϵ. The combination with a triangle inequality leads to

$$\begin{aligned}|w_H|_{H^1(\Omega)} &\geq \left|w_{H,\ell}\right|_{H^1(\Omega)} - \left|w_H - w_{H,\ell}\right|_{H^1(\Omega)} \\ &\geq (1 - \tilde{C}C(H,h,\epsilon,b,\ell)C_{I_H}\left(\tfrac{H}{h}\right)\beta^{\ell-1}) \left|w_{H,\ell}\right|_{H^1(\Omega)}.\end{aligned}$$

As $I_H(w_{H,\ell} - w_H) = 0$, i.e., $w_{H,\ell} - w_H \in R_H$, this leads to

$$\begin{aligned}|a(u_H, w_{H,\ell} - w_H)| &\leq \left(\epsilon + \|b\|_{L^\infty(\Omega)} H C_{I_H}\left(\tfrac{H}{h}\right)\right) |u_H|_{H^1(\Omega)} \left|w_{H,\ell} - w_H\right|_{H^1(\Omega)} \\ &= \epsilon \left(1 + \mathrm{Pe}_{H,b,\epsilon} C_{I_H}\left(\tfrac{H}{h}\right)\right) |u_H|_{H^1(\Omega)} \left|w_{H,\ell} - w_H\right|_{H^1(\Omega)}.\end{aligned}$$

The combination of the above displayed inequalities results in

$$\begin{aligned}a(u_H, w_{H,\ell}) &= a(u_H, w_H) + a(u_H, w_{H,\ell} - w_H) \\ &\geq \frac{\epsilon}{C_{I_H}\left(\frac{H}{h}\right)} (1 - \tilde{C} C(H, h, \epsilon, b, \ell) C_{I_H}\left(\tfrac{H}{h}\right) \beta^{\ell-1}) |u_H|_{H^1(\Omega)} \left|w_{H,\ell}\right|_{H^1(\Omega)} \\ &\quad - \epsilon (1 + \mathrm{Pe}_{H,b,\epsilon} C_{I_H}\left(\tfrac{H}{h}\right)) C(H, h, \epsilon, b, \ell) \tilde{C} C_{I_H}\left(\tfrac{H}{h}\right) \beta^{\ell-1} |u_H|_{H^1(\Omega)} \left|w_{H,\ell}\right|_{H^1(\Omega)}.\end{aligned}$$

Recall the definition of β from (4.6). If ℓ satisfies (5.10) then we obtain (5.11). □

We are ready to estimate the error $\left|u_H - u_{H,\ell}\right|_{H^1(\Omega)}$ coming from the localization.

LEMMA 5.6 Let ℓ satisfy (5.10). Then

$$\begin{aligned}\left|u_H - u_{H,\ell}\right|_{H^1(\Omega)} &\lesssim C_{I_H}\left(\tfrac{H}{h}\right)^2 C(H, h, \epsilon, b, \ell)(1 + \mathrm{Pe}_{H,b,\epsilon} C_{I_H}\left(\tfrac{H}{h}\right)) \\ &\quad \times \beta^{\ell-1} |u_h - u_H|_{H^1(\Omega)}. \end{aligned} \tag{5.14}$$

Proof. Notice that $u_H - u_{H,\ell} \in V_H$ is a coarse finite element function. Therefore, the inf–sup condition (5.12) guarantees the existence of $w_{H,\ell} \in W_{H,\ell}$ with

$$\left|u_H - u_{H,\ell}\right|_{H^1(\Omega)} \lesssim \frac{C_{I_H}\left(\frac{H}{h}\right)}{\epsilon} \frac{a(u_H - u_{H,\ell}, w_{H,\ell})}{\left|w_{H,\ell}\right|_{H^1(\Omega)}}.$$

In view of $w_{H,\ell} \in W_{H,\ell} \subset V_h$, the standard Galerkin problem (2.5) and the VMS method (5.9) imply

$$a(u_H - u_{H,\ell}, w_{H,\ell}) = a(u_H - u_h, w_{H,\ell}).$$

Define $w_H := I_H w_{H,\ell} - \mathcal{C}(I_H w_{H,\ell}) \in W_H \subset V_h$. Together with the orthogonality of Petrov–Galerkin type, we obtain

$$a(u_H - u_h, w_{H,\ell}) = a(u_H - u_h, w_{H,\ell} - w_H).$$

Taking into account that $w_{H,\ell} - w_H = (\mathcal{C} - \mathcal{C}_\ell) I_H w_{H,\ell}$, the combination with a Cauchy inequality, $w_{H,\ell} - w_H \in \ker(I_H)$ and an application of Theorem 5.2 lead to

$$a(u_H - u_h, w_{H,\ell} - w_H) \lesssim (\epsilon + \|b\|_{L^\infty(\Omega)} H C_{I_H}\left(\tfrac{H}{h}\right)) C(H, h, \epsilon, b, \ell) \beta^{\ell-1} \left|I_H w_{H,\ell}\right|_{H^1(\Omega)} |u_h - u_H|_{H^1(\Omega)}$$

The stability of I_H from (3.1) implies the assertion.

Lemma 5.6 allows us to bound the error for the localized VMS method in the following manner.

THEOREM 5.7 (Global error estimate for the localized VMS method) Let ℓ satisfy (5.10); then

$$\left|u_h - u_{H,\ell}\right|_{H^1(\Omega)} \lesssim \left(C_{I_H}\left(\tfrac{H}{h}\right) + C_{I_H}\left(\tfrac{H}{h}\right)^3 C(H,h,\epsilon,b,\ell)(1+\mathrm{Pe}_{H,b,\epsilon}\, C_{I_H}\left(\tfrac{H}{h}\right))\beta^{\ell-1}\right) \times \min_{v_H \in V_H} |u_h - v_H|_{H^1(\Omega)}$$

with the constant $C(H,h,\epsilon,b,\ell)$ from (5.7).

Proof. The proof follows directly from a triangle inequality, Proposition 3.1 and Lemma 5.6.

Although Theorem 5.7 provides a best approximation result, the assertion still depends on ϵ, which is hidden in the best approximation $\min_{v_H \in V_H} |u_h - v_H|_{H^1(\Omega)}$. The locality in the error bound of the ideal method from Proposition 3.1 transfers to the VMS method defined in (5.9) and results in the local error bound in the following theorem. Note that the error from the localization still depends on the mesh Péclet number of $\mathcal{T}_H$ and still contains the best approximation error on the whole domain. Nevertheless, these ill-behaved terms are weighted by the exponentially decaying term $\beta^{\ell-1}$, where β is bounded above from 1.

THEOREM 5.8 (Local error estimate for the localized VMS method) Let ℓ satisfy (5.10). Then for any $\mathcal{K} \subset \mathcal{T}_H$ and $\omega := \cup\mathcal{K}$, it holds that

$$\left|u_h - u_{H,\ell}\right|_{H^1(\omega)} \lesssim C_{I_H}\left(\tfrac{H}{h}\right) \min_{v_H \in V_H} |u_h - v_H|_{H^1(\omega)} + C_{I_H}\left(\tfrac{H}{h}\right)^3 C(H,h,\epsilon,b,\ell)(1+\mathrm{Pe}_{H,b,\epsilon}\, C_{I_H}\left(\tfrac{H}{h}\right))\beta^{\ell-1} \min_{v_H \in V_H} |u_h - v_H|_{H^1(\Omega)}\,.$$

REMARK 5.9 (Complexity) Problem (5.9) on the coarse scale consists of $\mathcal{O}(1/H^2)$ degrees of freedom (DOFs). Corresponding to each of those DOFs, one localized corrector problem (5.1) has to be solved, which relates to $\mathcal{O}(\ell^2 H^3/(h^2\epsilon))$ DOFs in the worst-case scenario. If the mesh is structured, the number of corrector problems that have to be solved can be reduced to $\mathcal{O}(\ell H/\epsilon)$ (cf. Gallistl & Peterseim, 2015).

6. Numerical experiment

In this section, we present one simple numerical test to illustrate the theoretical convergence results of the localized method proposed in (5.9). We take $\Omega = (0,1)\times(0,1)$, the velocity field $b = (\cos(0.7), \sin(0.7))^{\mathrm{T}}$, the volume force $f \equiv 1$ and $\epsilon = 2^{-7}$. The reference solution u_h is obtained through (2.5) by taking $h = \sqrt{2}\,2^{-8}$.

We will compare our approach with the SUPG method. Let us briefly review the SUPG model to (1.1) (Franca *et al.*, 1992). Let $(\bullet,\bullet)_T := (\bullet,\bullet)_{L^2(T)}$ denote the L^2 scalar product over a triangle $T \in \mathcal{T}_H$. Then the SUPG method seeks $u_H \in V_H$ such that

$$B_{\mathrm{SUPG}}(u_H^{\mathrm{SUPG}}, v_H) = F_{\mathrm{SUPG}}(v_H) \qquad \text{for all } v_H \in V_H \tag{6.1}$$

with

$$B_{\mathrm{SUPG}}(u_H^{\mathrm{SUPG}}, v_H) = a(u_H^{\mathrm{SUPG}}, v_H) + \delta_{\mathrm{SUPG}} \sum_{T \in \mathcal{T}_H} (b \cdot \nabla u_H^{\mathrm{SUPG}}, b \cdot \nabla v_H)_T$$

and

$$F_{\mathrm{SUPG}}(v_H) = \langle f, v_H \rangle_{H^{-1}(\Omega) \times H_0^1(\Omega)} + \delta_{\mathrm{SUPG}} \sum_{k \in \mathcal{T}_H} (f, b \cdot \nabla v_H)_T.$$

Here, δ_{SUPG} indicates the stability parameter, and we choose

$$\delta_{\mathrm{SUPG}} = \frac{H}{\sqrt{8}\max(\epsilon, H/\sqrt{2})}$$

in our numerical test.

The reference solution from (2.5) and the coarse-scale solution from (5.9) and the SUPG solution from (6.1) with $H = \sqrt{2}\,2^{-4}$ are depicted in Fig. 6. One can observe that the classical FEM approximation with $H = \sqrt{2}\,2^{-4}$ is not stable around the boundary layers (i.e., the top and right boundaries) and shows spurious oscillations and thus fails to provide a reliable solution. Nevertheless, both the SUPG method and the ideal method are stable and generate an accurate solution. In Fig. 7, we display the solutions for fixed $y = 0.75$ to illustrate the stability and accuracy of the VMS method. We observe large oscillations in the coarse-scale solution obtained through classical FEM when x approaches 1, while the SUPG and the VMS methods yield reliable solutions. The smearing is restricted to one layer of elements around the boundary. We can also conclude that the SUPG and the VMS methods reproduce the reference solution away from $x = 1$ and the latter shows slightly less smearing. We want to highlight that the localization parameter is $\ell = 1$ for the VMS method in this example.

Tables 1 and 2 list the errors between the localized solutions (5.9) and the reference solution u_h under various coarse mesh sizes H and localization parameters ℓ. We observe an optimal convergence rate of $\mathcal{O}(H)$ in Table 1 for the error in the H^1 seminorm in the domain $[0, 0.75] \times [0, 0.75]$ away from the boundary layers and an optimal convergence rate of $\mathcal{O}(H^2)$ in Table 2 for the global error in the L^2 norm. Although Theorem 5.8 guarantees optimality only under the assumption that ℓ is large enough in the sense of (5.10), the numerical experiment demonstrates that $\ell = 1$ is sufficient for an accurate solution, which implies a potentially huge computational reduction.

The convergence rate for $u_{H,1}$ with various ϵ in a range from 2^{-5} to 2^{-8} is shown in Figs 8 and 9. The error is stable and of order $\mathcal{O}(H)$ with respect to the H^1 seminorm in a region away from boundary layers and of order $\mathcal{O}(H^2)$ in the global L^2 norm with a preasymptotic effect for smaller values of ϵ. For comparison, the nodal interpolation error (i.e., the error from the ideal method) in the global L^2 norm is depicted, which agrees with $\|u_h - u_{H,1}\|_{L^2(\Omega)}$ very well. This justifies the fast convergence of the localized method with respect to the localization parameter ℓ for all of the considered values of ϵ.

7. Conclusions

In this article, a singularly perturbed convection–diffusion equation was considered, and we obtained a stable locally quasi-optimal variational multiscale method based on the nodal interpolation operator. Because of the high complexity involved in solving the global correctors, which account for the main component of the VMS method, a further model reduction was proceeded by localization techniques

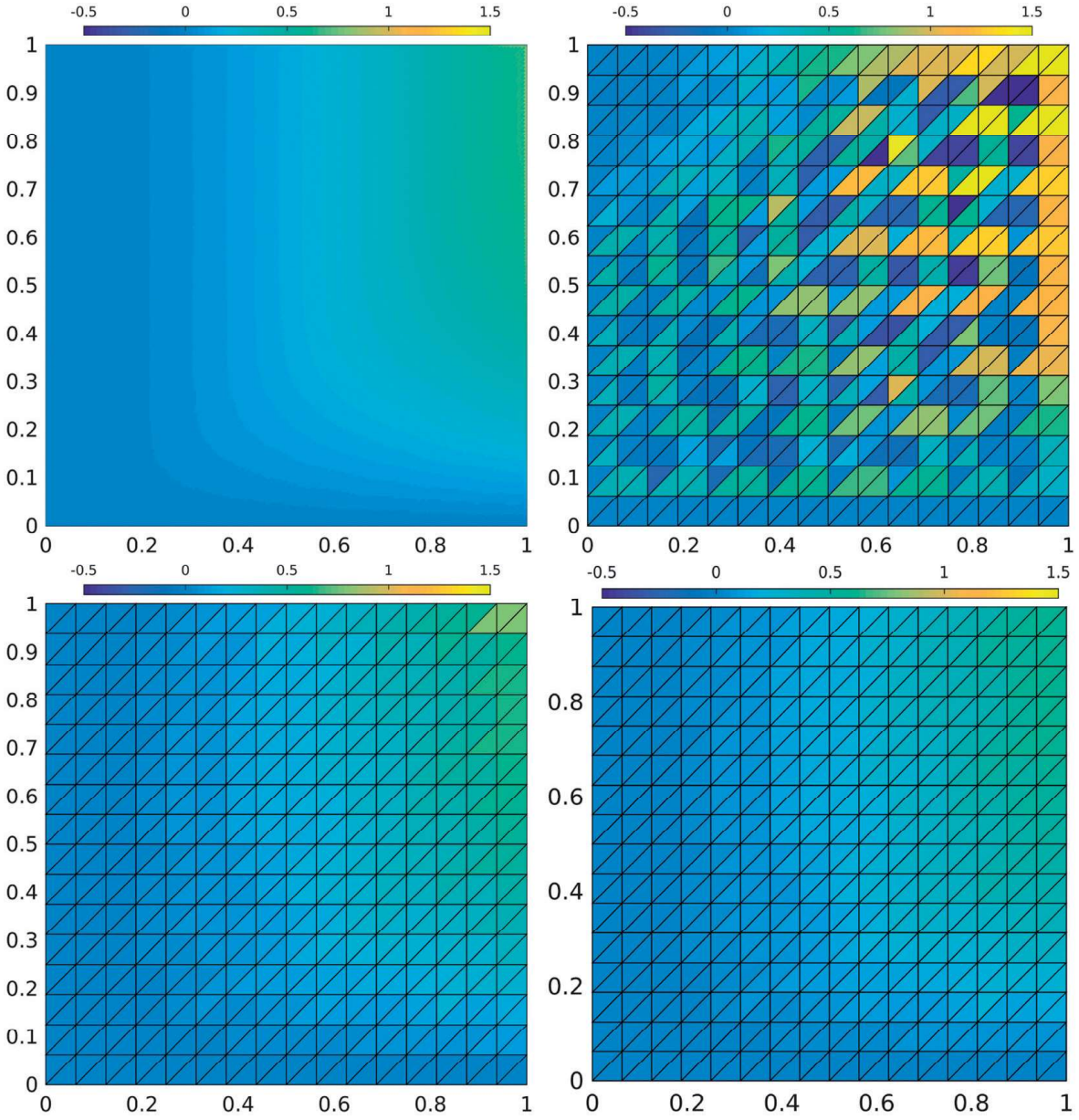

FIG. 6. Reference solution (top left), classical FEM approximation (top right), SUPG approximation (bottom left) and multiscale approximation for $\ell = 1$ (bottom right) for $\epsilon = 2^{-7}$ and $H = \sqrt{2}\,2^{-4}$.

based on the LOD method. This localization employs local patches that depend on the velocity field b and the singular perturbation parameter ϵ. The error of the localization decays exponentially. We also provided a numerical experiment to illustrate our theoretical results.

The stability constant of the nodal interpolation operator that occurs in the error estimate depends logarithmically on H/h (and so on ϵ). In the three-dimensional case, this stability estimate depends polynomially on H/h. Therefore, a generalization of the proposed method to three dimensions does not seem reasonable.

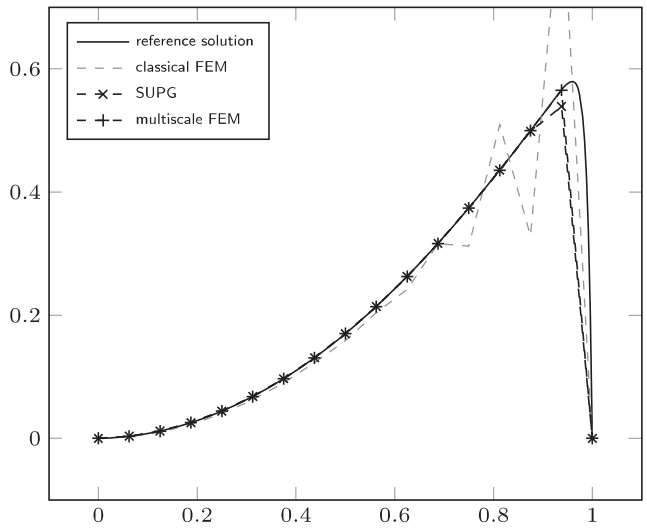

FIG. 7. Reference solution, classical FEM, SUPG and multiscale approximation for $\ell = 1$ at the line $y = 0.75$ on a mesh with mesh size $H = \sqrt{2}\,2^{-4}$ for $\epsilon = 2^{-7}$.

TABLE 1 *The error* $\|\nabla(u_h - u_{H,\ell})\|_{L^2(\Omega_r)}$ *for* $\Omega_r = [0, 0.75] \times [0, 0.75]$ *for different localization parameters* ℓ *and mesh sizes* H *for* $\epsilon = 2^{-7}$

	$\ell = 1$	$\ell = 2$	$\ell = 3$	$\ell = 4$	$\ell = 5$	$\ell = 6$
$H = \sqrt{2}\,2^{-3}$	5.14e−02	5.14e−02	5.14e−02	5.14e−02	5.14e−02	5.14e−02
$H = \sqrt{2}\,2^{-4}$	2.57e−02	2.57e−02	2.57e−02	2.57e−02	2.57e−02	2.57e−02
$H = \sqrt{2}\,2^{-5}$	1.27e−02	1.27e−02	1.27e−02	1.27e−02	1.27e−02	1.27e−02
$H = \sqrt{2}\,2^{-6}$	6.23e−03	6.23e−03	6.23e−03	6.23e−03	6.23e−03	6.23e−03

TABLE 2 *The error* $\|u_h - u_{H,\ell}\|_{L^2(\Omega)}$ *for different localization parameters* ℓ *and mesh sizes* H *for* $\epsilon = 2^{-7}$

	$\ell = 1$	$\ell = 2$	$\ell = 3$	$\ell = 4$	$\ell = 5$	$\ell = 6$
$H = 0.17678$	9.45e−02	9.45e−02	9.45e−02	9.45e−02	9.45e−02	9.45e−02
$H = 0.088388$	5.34e−02	5.34e−02	5.34e−02	5.34e−02	5.34e−02	5.34e−02
$H = 0.044194$	2.31e−02	2.32e−02	2.32e−02	2.32e−02	2.32e−02	2.32e−02
$H = 0.022097$	7.25e−03	7.27e−03	7.27e−03	7.27e−03	7.27e−03	7.27e−03

The local patches in the localized computation of the corrector depend on ϵ. It is an open question whether this is optimal or whether a further reduction or simplification is possible.

Acknowledgements

This article has been written on the occasion of the trimester program on multiscale problems of the Hausdorff Institut for Mathematics (Bonn).

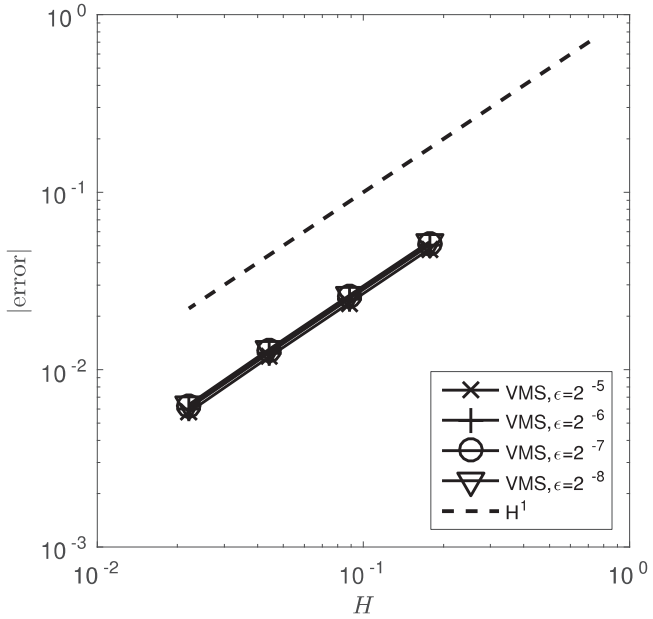

FIG. 8. The errors $\|\nabla(u_h - u_{H,1})\|_{L^2(\Omega_r)}$ for $\Omega_r = [0, 0.75] \times [0, 0.75]$ for different values of ϵ.

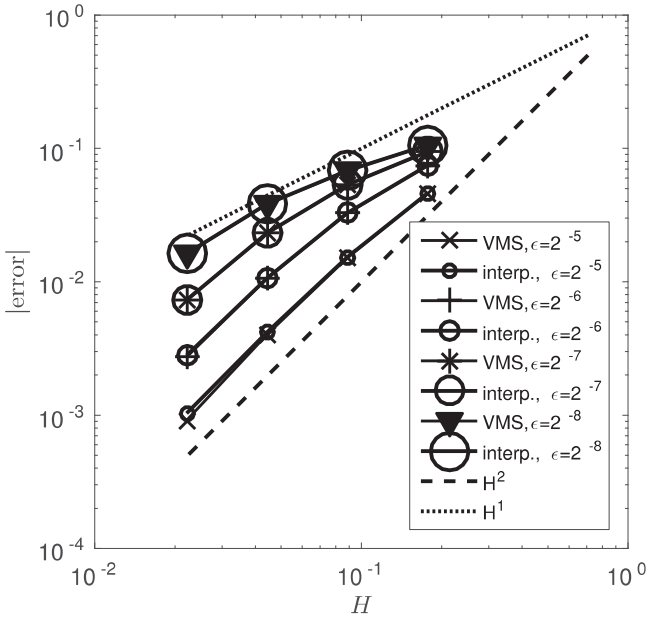

FIG. 9. The errors $\|u_h - u_{H,1}\|_{L^2(\Omega)}$ and $\|u_h - I_H u_h\|_{L^2(\Omega)}$ for different values of ϵ.

Funding

Hausdorff Center for Mathematics Bonn (to G.L.). Deutsche Forschungsgemeinschaft in the Priority Program 1748 'Reliable simulation techniques in solid mechanics: Development of nonstandard discretization methods, mechanical and mathematical analysis' under the project 'Adaptive isogeometric modeling of propagating strong discontinuities in heterogeneous materials' (PE2143/2-1; to D.P.).

References

Barrenechea, G. R., Burman, E. & Karakatsani, F. (2016) Edge-based nonlinear diffusion for finite element approximations of convection–diffusion equations and its relation to algebraic flux-correction schemes. *Numer. Math.*, **135**, 521–545.

Brezzi, F., Marini, D. & Süli, E. (2000) Residual-free bubbles for advection-diffusion problems: the general error analysis. *Numer. Math.*, **85**, 31–47.

Calo, V. M., Chung, E. T., Efendiev, Y. & Leung, W. T. (2016) Multiscale stabilization for convection-dominated diffusion in heterogeneous media. *Comput. Methods Appl. Mech. Eng.*, **304**, 359–377.

Cangiani, A. & Süli, E. (2005a) Enhanced RFB method. *Numer. Math.*, **101**, 273–308.

Cangiani, A. & Süli, E. (2005b) Enhanced residual-free bubble method for convection-diffusion problems. *Int. J. Numer. Methods Fluids*, **47**, 1307–1313. 8th ICFD Conference on Numerical Methods for Fluid Dynamics. Part 2.

Christiansen, S., Halvorsen, T. & Sørensen, T. (2016) Stability of an upwind Petrov-Galerkin discretization of convection diffusion equations. ArXiv e-prints, arXiv:1406.0390v2.

Codina, R. (2000) Stabilization of incompressibility and convection through orthogonal sub-scales in finite element methods. *Comput. Methods Appl. Mech. Eng.*, **190**, 1579–1599.

Demkowicz, L., Gopalakrishnan, J. & Niemi, A. H. (2012) A class of discontinuous Petrov-Galerkin methods. Part III: adaptivity. *Appl. Numer. Math.*, **62**, 396–427.

Elfverson, D. (2015) A discontinuous Galerkin multiscale method for convection-diffustion problems. ArXiv e-prints.

Franca, L. P., Frey, S. L. & Hughes, T. J. (1992) Stabilized finite element methods: I. Application to the advective-diffusive model. *Comput. Methods Appl. Mech. Eng.*, **95**, 253–276.

Gallistl, D. & Peterseim, D. (2015) Stable multiscale Petrov-Galerkin finite element method for high frequency acoustic scattering. *Comp. Meth. Appl. Mech. Eng.*, **295**, 1–17.

Harder, C., Paredes, D. & Valentin, F. (2015) On a multiscale hybrid-mixed method for advective-reactive dominated problems with heterogeneous coefficients. *Multiscale Model. Simul.*, **13**, 491–518.

Hughes, T. J. R. & Sangalli, G. (2007) Variational multiscale analysis: the fine-scale Green's function, projection, optimization, localization, and stabilized methods. *SIAM J. Numer. Anal.*, **45**, 539–557.

John, V. & Schmeyer, E. (2009) On finite element methods for 3D time dependent convection-diffusion-reaction equations with small diffusion. *BAIL 2008 - boundary and interior layers*, 173–181, Lecture Notes in Computational Science and Engineering, 69, Berlin: Springer.

Larson, M. G. & Målqvist, A. (2009) An adaptive variational multiscale method for convection-diffusion problems. *Comm. Numer. Methods Eng.*, **25**, 65–79.

Målqvist, A. & Peterseim, D. (2014) Localization of elliptic multiscale problems. *Math. Comp.*, **83**, 2583–2603.

Melenk, J. M. (1997) On the robust exponential convergence of *hp* finite element methods for problems with boundary layers. *IMA J. Numer. Anal.*, **17**, 577–601.

Melenk, J. M. (2002) *hp-Finite Element Methods for Singular Perturbations*. Lecture Notes in Mathematics, vol. 1796. Berlin: Springer.

Park, P. J. & Hou, T. Y. (2004) Multiscale numerical methods for singularly perturbed convection-diffusion equations. *Int. J. Comput. Methods*, **1**, 17–65.

Peterseim, D. (2017) Eliminating the pollution effect in Helmholtz problems by local subscale correction. *Math. Comp.*, **86**, 1005–1036.

Peterseim, D. (2016b) Variational multiscale stabilization and the exponential decay of fine-scale correctors. *Building Bridges: Connections and Challenges in Modern Approaches to Numerical Partial Differential Equations* (Barrenechea, G. R., Brezzi, F., Cangiani, A. & Georgoulis, E. H. eds). Lecture Notes in Computational Science and Engineering, vol. 114. Cham: Springer, pp. 343–369.

Qiu, W. & Shi, K. (2015) An HDG method for convection diffusion equation. *J. Sci. Comput.*, **66**, 346–357.

ROOS, H., STYNES, M. & TOBISKA, L. (2008) *Robust Numerical Methods for Singularly Perturbed Differential Equations: Convection-Diffusion-Reaction and Flow Problems*. Springer Series in Computational Mathematics, 24. Berlin: Springer-Verlag.

YSERENTANT, H. (1986) On the multilevel splitting of finite element spaces. *Numer. Math.*, **49**, 379–412.